Tao, Y., An, L., Xiao, F., Lia, G, Ding, Y, Paul, M. J. and Liu, Z. 2022. Integration of embryo–endosperm interaction into a holistic and dynamic picture of seed development using a rice mutant with notched-belly kernels. *The Crop Journal.* 10, pp. 729-742. https://doi.org/10.1016/j.cj.2021.10.007

The Crop Journal 10 (2022) 729–742

Contents lists available at ScienceDirect

The Crop Journal

journal homepage: www.keaipublishing.com/en/journals/the-crop-journal/

Integration of embryo–endosperm interaction into a holistic and dynamic picture of seed development using a rice mutant with notched-belly kernels

Yang Tao [a], Lu An [a], Feng Xiao [a], Ganghua Li [a], Yanfeng Ding [a], Matthew J. Paul [b], Zhenghui Liu [a,c,*]

[a] College of Agriculture, Nanjing Agricultural University, Nanjing 210095, Jiangsu, China
[b] Plant Science, Rothamsted Research, Harpenden, Hertfordshire, AL5 2JQ, UK
[c] Collaborative Innovation Center for Modern Crop Production, Nanjing Agricultural University, Nanjing 210095, Jiangsu, China

ARTICLE INFO

Article history:
Received 14 July 2021
Revised 28 September 2021
Accepted 28 October 2021
Available online 6 December 2021

Keywords:
Seed development
Embryo–endosperm interaction
Developmental transition
Transcriptome
Sugar signaling
Rice physiology

ABSTRACT

Interaction between the embryo and endosperm affects seed development, an essential process in yield formation in crops such as rice. Signals that mediate communication between embryo and endosperm are largely unknown. We used the notched-belly (NB) mutant with impaired communication between embryo and endosperm to investigate the effect of the embryo on developmental staging of the endosperm and signaling pathways in the embryo that regulate endosperm development. Hierachical clustering of mRNA datasets from embryo and endosperm samples collected during development in NB and a wild type showed a delaying effect of the embryo on the developmental transition of the endosperm by extension of the middle stage. K-means clustering further identified coexpression modules of gene sets specific to embryo and endosperm development. Combined gene expression and biochemical analysis showed that T6P–SnRK1, gibberellin and auxin signaling by the embryo regulate endosperm developmental transition. We propose a new seed developmental staging system for rice and identify the most detailed signature of rice grain formation to date. These will direct genetic strategies for rice yield improvement.

1. Introduction

The seed (kernel) of rice (*Oryza sativa*) is a complex but delicate biological system, containing three genetically distinct tissues: diploid embryo, triploid endosperm, and diploid maternal tissues [1]. Rice is a main contributor of dietary calories and nutrients for nearly half of the global population [2]. Rice grain yield must be sustainably improved both in quantity and quality, to solve formidable challenges including the ever-increasing population, climate change, and the quest for high-quality rice that has accompanied the rise in living standards [3]. A detailed understanding of the molecular and physiological mechanisms underpinning seed development may permit the design of effective strategies to boost rice quality and yield.

Milled rice is the main form of rice for consumption. It is produced by milling, during which the outer maternal layers, the embryo, the aleurone, and part of the starchy endosperm are removed. End-use quality of rice seed is thus dominated by the physico-chemical properties of endosperm, which is packed with starch granules and protein bodies [4]. Most research on rice quality has been centered on the starchy endosperm, revealing that its development is controlled by multiple genes and by environmental conditions [5–7].

The composition, structure, and size of endosperm are affected by its interactions with other tissues, in particular the embryo, throughout seed development. Endosperm provides nutrients to drive embryo growth and physically restrains its size and development. The embryo is the germline component of the seed, and affects the allocation of sugars and other nutrients such as amino acids and minerals to the endosperm. Concomitant development of embryo and endosperm under the constraint of maternal tissues (seed coat or pericarp) requires coordination of the two compartments [8,9]. Growing evidence in rice as well as *Arabidopsis thaliana* and maize (*Zea mays*) supports bidirectional communication between embryo and endosperm, as reviewed by Lafon-Placette and Köhler [8], An et al. [1], and Ingram [10]. Thus,

* Corresponding author.
E-mail address: liuzh@njau.edu.cn (Z. Liu).

https://doi.org/10.1016/j.cj.2021.10.007

both embryo and endosperm and their interaction affect grain filling and quality.

Transcriptome analyses of seed development have identified most genes expressed in the two compartments [11]. These comprehensive studies have identified molecular networks and pathway interactions that function during the development of individual seed compartments in *Arabidopsis* [12], maize [13,14], wheat (*Triticum aestivum*) [15], and barley (*Hordeum vulgare*) [16]. In rice, Ishimaru et al. [7] isolated the aleurone, dorsal, central, and lateral tissues of developing endosperm by laser-capture microdissection (LCM), and profiled their gene expression with a 44 K microarray, revealing that high-molecular-weight heat-shock proteins have a role in mediating redox, nitrogen and amino acid metabolism in chalky tissue under heat stress. Wu et al. [2] profiled gene expression activity in the nucellar epidermis, ovular vascular trace, endosperm, and aleurone at three distinct grain development stages, unraveling some molecular aspects of grain development. Ram et al. [17] employed a rapid LCM approach to collect pericarp, aleurone, embryo, and endosperm at 10 days after anthesis (DAF). Subsequent RNA-seq analysis identified 7760 differentially expressed genes, from which the authors inferred key tissue-specific pathways responsible for nutrient partitioning. However, these studies do not permit an integrated understanding of the cellular processes governing the formation of rice grain, because of the scarcity of information on embryo–endosperm communication and its influence on rice yield and quality. This scarcity is due partly to the complexity of seed structures [9].

Notched-belly grain is a misshapen type of rice kernel, having a notched-line on the ventral side and thus being inferior in appearance and milling quality [18]. Previously, we identified a notched-belly mutant (NB) of a japonica rice, Wuyujing 3, using a chemical mutagen [19]. It has a high incidence of white-belly kernel, and the notched line, visible at 5 DAF, separates the endosperm into two subcompartments, the translucent upper part and the chalky lower part (Fig. 1). Given that the formation of chalky tissue is a result of incomplete accumulation of starch and protein, it is tempting to speculate that the embryo plays a role in it, probably by depriving the adjacent lower endosperm of nutrients [1]. As revealed by our previous studies [6,20], the embryo reduced the contents of proteins, amino acids, and minerals in the chalky endosperm. Thus, the NB mutant permits an integrated understanding of the cellular processes for rice grain formation from a perspective of embryo–endosperm interaction. In this study, we used the NB mutant to characterize the genome-wide gene expression profile of embryo and endosperm samples between 0 and 60 DAF. In combination with physiological and histological investigations, we aimed to: (i) characterize the effect of the embryo on endosperm development; and (ii) frame a holistic and dynamic picture of seed development by integrating information of embryo–endosperm crosstalk.

2. Materials and methods

2.1. Plant materials and sampling

The notched-belly mutant (NB) was obtained by Ethyl methane sulfonate (EMS) treatment of a japonica rice cultivar, Wuyujing 3 (WT). It shows a high proportion of notched-belly kernels with a white belly mainly on the lower endosperm [19]. In 2018, six seedlings of WT and NB were transplanted into a plastic pot filled with 10 kg paddy soil. The plants were grown under natural conditions, and at two days before flowering were transferred to a 31/24 °C growth chamber (12/12 h day and night cycle), with light intensity of 600 μmol photons m^{-2} s^{-1} and relative humidity 70% ± 5%. Flowering dates were recorded for sampled caryopses on the middle primary rachis. Kernels were sampled at eight times: 5, 10, 15, 20, 25, 30, 45, and 60 DAF, with three biological replicates. Samples were quickly frozen in liquid nitrogen and then stored at − 80 °C

Fig. 1. Overview of a time series samples of embryo and endosperms. Dotted line indicates the manual dissection of endosperm, cutting it into upper and lower endosperms. DAF, days after fertilization; E, embryo; En, endosperm; EnL, lower part of endosperm; EnU, upper part of endosperm; NB, notched-belly rice mutant; WT, wild type of Wuyujing 3. Scale bar, 1 mm.

until analysis. The developing kernels were manually dissected into three subsamples: the embryo and the upper and lower parts of the endosperm (Fig. 1). Endosperm samples contain the maternal tissues of pericarp and seed coat.

2.2. Gene expression profiling by RNA-seq

A 0.1 g sample was used for total RNA extraction with TRIzol reagent (Invitrogen, Carlsbad, CA, USA). The extracted RNA was dissolved in 100 μl of RNase-free water and quantified with a NanoDrop spectrophotometer (Thermo Scientific, Waltham, MA, USA). RNA quality was evaluated using the 6000 Pico LabChip of the Agilent 2100 Bioanalyzer (Agilent, Santa Clara, CA, USA). Quality checking and quantification of the sample library were performed with an Agilent 2100 Bioanaylzer and StepOnePlus Real-Time PCR System (Applied Biosystems, Waltham, MA, USA). Library products were sequenced with BGISEQ-500 platform (BGI, Shenzhen, China). The Nipponbare reference genome (IRGSP-1.0; https://www.ncbi.nlm.nih.gov/genome/?term=IRGSP-1.0) was used to process the RNA-seq libraries into read mapping and analysis.

To ensure good quality and effective mapping, low-quality reads were removed with SOAPnuke (1.4.0) [21]and Trimmomatic (0.36) [22], and only clean reads were processed for mapping using HISAT2 (2.1.0) [23]. Gene expression levels were measured with RSEM (1.2.8) [24], and fragments per kilobase of transcript per million mapped reads (FPKM) values were used for quantifying gene activity. Only genes with FKPM $\geq$ 1 were considered as expressed, to eliminate the influence of transcriptomic noise. To confirm the accuracy and authenticity of the three biological repeats, Pearson correlation coefficients among them were calculated with the normalized expression level of $\log_2$ (FPKM value + 1) (Fig. S1). Differentially expressed genes (DEGs) were accepted if they exhibited an absolute value of $\log_2$ ratio $\geq$ 1 compared with an FDR-corrected *P*-value of $\leq$ 0.001 [25].

2.3. Validation of transcriptome data using qRT-PCR

RNA-seq data quality was validated by measuring the relative expression patterns of 12 genes functioning in C and N metabolism using qRT-PCR (Fig. S2). Target-specific qRT-PCR primers were designed with Primer5.0 software [26] and synthesized, as described in Table S1. Each sample was represented by three biological and three technical replicates. Comparison of qRT-PCR results with RNA-seq revealed similar expression patterns in the two datasets, validating the transcriptomic data (Fig. S2). The transcript abundance patterns of embryo (*OSH1* and *OsLEC1*) and endosperm *(GluD-1* and *RPBF)* specific genes also confirmed the credibility of the gene expression data (Fig. S3), indicating that the embryo and endosperm samples were processed well.

2.4. PCA and hierarchical clustering

To facilitate graphical interpretation of relatedness among the 48 tissue samples, the dimensional expression data were reduced to two dimensions by PCA using Omicshare tools (https://www.omicshare.com/tools/Home/Soft/pca). Hierarchical clustering (HCL) was performed with the same software.

2.5. Gene coexpression and functional enrichment analysis

Coexpression analysis for genes in embryo and endosperm was performed with MeV [27]. The Z-score was used to calculate the relative expression levels before running the MeV for a tissue. These Z-scores were used as input for MeV and each individual dataset was clustered using the k-means method and Pearson correlation coefficients among the genes. Using Gene Ontology (GO) annotation, genes were assigned to functional categories [28]. Functional enrichment analysis was performed using the phyper function in R with default setting [29]. *P*-value was used as a filter to identify significant (*P*-value < 0.01) GO categories. Embryo- or endosperm-specific genes were identified by Z-score. A gene was determined to be embryo-specific if it had a Z-score above 2 in at least one of the embryo samples compared with the endosperm samples. Similarly, a gene was determined to be endosperm-specific if it had a Z-score above 2 in at least one of the endosperm samples compared with the embryo samples.

2.6. Light microscopy observation of grain structure

Grains samples were fixed immediately in 0.1 mol L^{-1} phosphate buffer solution (pH 7.2), containing 2.5% glutaraldehyde (v/v) and 2% paraformaldehyde (w/v). They were then dehydrated in a graded ethanol series, transferred to acetone, and embedded in low-glutinosity Spurr's resin (Spurr Low-Viscosity Embedding Kit, Sigma-Aldrich, Saint Louis, MO, USA). The samples were polymerized at 70 °C for 8 h. Semi-thin sections (2 μm) were cut in the longitudinal plane (embryo) and the transverse plane (endosperm) of the kernels, using a Leica Ultrathin Microtome EM UC7 (Leica, Wetzlar, Germany). Samples were stained with 1% methyl violet and observed and photographed under a BX53 light microscope (Olympus, Tokyo, Japan).

2.7. Chemical analysis for metabolites

Sucrose, fructose, glucose, and starch: sugar contents were measured by ultra-high performance liquid chromatography (UHPLC) following Chen et al. [30]. Sucrose and hexoses were extracted with 80% (v/v) ethanol for 30 min at 80 °C, followed by centrifugation at 5000×*g* for 15 min. The supernatant was pooled and lyophilized using a Maxi-Dry Lyo instrument (Heto-Holten, Wettenberg, Germany), and resuspended in ultrapure water and filtered through a 0.45 μm pore-size filter. The filtrate was loaded into a Dionex Ultimate 3000 chromatography system. Starch content was measured using anthrone reagent at wavelength of 620 nm, after extraction by ethanol and digestion by perchloric acid.

T6P and SnRK1 activity: T6P was extracted and purified following Delatte et al. [31], and quantified by ultra-performance liquid chromatography (ACQUITY UPLC I-Class PLUS, Waters, Milford, MA, USA) coupled with a triple quadruple mass spectrometry system (Xevo TQ-S micro, Waters, Milford, MA, USA), following Sastre Toraño et al. [32]. SnRK1 was extracted and its activity was assayed following Zhang et al. [33], using AMARA peptide as substrate.

Amino acids and proteins: samples were boiled with 80% ethanol until fully bleached to extract free amino acids (FAAs). Centrifuged for 15 min, the supernatant was pooled and filtered through a 0.45 μm pore-size filter, and then used for FAA determination with an amino acid analyzer (L-8900, Hitachi, Tokyo, Japan). Protein fractions including albumin, globulin, prolamin, and glutelin were extracted and measured following Ning et al. [34].

Phytohormones and minerals: IAA, ABA, CKs (tZ and tZR) and GAs (GA_1, GA_3, GA_4, and GA_7) were extracted and purified following Wu et al. [35]. IAA, ABA, and CKs were quantified by ultra-performance liquid chromatography according to Chou et al. [36]. GAs were quantified by ultra-high performance liquid chromatography (AGILENT 1290, Agilent Technologies, Santa Clara, CA, USA) coupled with mass spectrometry (SCIEX-6500 Qtrap, AB SCIEX, Los Angeles, CA, USA). Minerals, including P, K, Ca, Na, Mg, Fe, Zn, Mn, and Cu, were quantified by inductively coupled plasma optical emission spectrometry (ICP-OES 710, Agilent Technologies, Santa Clara, CA, USA), following Wang et al. [37].

2.8. Statistical analysis

The concentration data of metabolites presented in the study are averages of triplicate observations. Significant analysis was performed with SPSS statistics package (19.0, SPSS Inc., Chicago, IL, USA) statistical software. Multiple comparisons were evaluated by Duncan's multiple range test ($P < 0.05$). Origin (9.0, OriginLab Inc., Northampton, MA, USA) was used for plotting.

3. Results

3.1. The generation and analysis of transcriptome data of developing embryo and endosperm

A total of 20,820 genes were expressed in at least one of the 48 samples. Among them, 18,171 genes were expressed in both embryo and endosperm, while only 1969 and 680 genes were expressed specifically in embryo and endosperm, respectively (Fig. 2A). mRNA datasets from different tissues were compared to reveal individual characteristics of the embryo and endosperm during seed development. Most genes were expressed in seed tissues during the early developmental phase (Fig. 2B). Within the endosperm, both genotypes showed higher gene activity in the upper part of the endosperm (EnU) than the lower part (EnL) (Fig. 2C). Embryo samples showed more expressed genes than endosperm throughout seed development (Fig. 2B).

3.2. Categorizing developmental processes of embryo and endosperm based on gene expression pattern

PCA distinguished the samples into two distinct groups based on tissue identity, validating the purity of the tissue samples (Fig. 2D). In particular, the first component (PC1; 77.1% variance explained) clearly separated the embryo from endosperm samples, while the second component (PC2; 12.6% variance explained) discriminated among developmental stages. The transcriptomic data in dendrograms were further classified by HCL, revealing four distinct groups within embryo and endosperm, with each group corresponding to a specific developmental stage (Fig. 2E–H).

For embryo samples, the two genotypes showed almost identical dendrograms (Fig. 2E, F). The first cluster is formed at 5 DAF, representing the stage around differentiation (Em-S1). During this stage, coleoptile and shoot apical meristem emerge and first leaf primordium becomes visible on the opposite side of the coleoptiles, as visualized by electron microscopy (Fig. S4). The second cluster from 10 to 15 DAF represents the embryo enlargement stage (Em-S2), as characterized by the formation of second and third leaf primordia, and organ enlargement (particularly of the scutellum). The third cluster at 20 DAF corresponds to the maturation phase (Em-S3) and shows no marked morphological change. The fourth cluster from 25 to 60 DAF represents the period of seed dormancy (Em-S4).

By contrast, the duration of developmental stages in endosperm varied by genotype. First, endosperms from WT showed four primary clusters (Fig. 2G, H), but those from NB showed only three clusters, suggesting abnormal development during the middle and later stages (Fig. 2I, J). Second, within the endosperm, the upper and lower parts of WT showed identical duration. However, for NB, the time span of endosperm filling in the lower endosperm (NB_EnL) was prolonged (15–25 DAF), relative to the upper endosperm (NB_EnU), the duration of whose second cluster (15–20 DAF) was identical to that of the WT. Consequently, the maturation and dormancy stage were delayed in the lower endosperm and displayed as a merged cluster (30–60 DAF) of stages 3 and 4, in contrast to the upper part, where stages 3 and 4 cluster had the same duration (25–60 DAF) as WT. Collectively, these findings indicated a disturbance in the developmental process of the lower endosperm of NB as a result of its proximity to the embryo.

The normal type of WT instead of the disturbed NB was used for a general description of the developmental signatures of the rice kernel. The four clearly defined clusters in WT endosperm show that the differentiation (En-S1) stage lasts from 5 to 10 DAF in which cellularization is completed, with the aleurone cells starting to become morphologically distinct from the starchy endosperm (Fig. S4). The storage accumulation stage (En-S2) occurs at 15–20 DAF, followed by the maturation (En-S3) phase of the endosperm at 25–30 DAF. The biological processes involved in dormancy (En-S4) are induced from 45 to 60 DAF. Together, these results showed a divergent staging mechanism of developmental events between embryo and endosperm.

3.3. Coexpressed gene sets of embryo and endosperm development

WT (Fig. 3A, B) and NB (Fig. 3A', B') shared a similar pattern of coexpression module. Accordingly, the normal type of WT was used for representation. Twenty-two coexpression modules were generated for both embryo and endosperm of WT. Among these modules, 11 and 9 were expressed broadly at more than one stage in embryo and endosperm, respectively, indicating some cellular processes common to several stages. Genes from the 11 modules of embryo and the 13 modules of endosperm were more prevalent at one of the four developmental stages, indicating specific functions of these modules at the corresponding stages.

3.3.1. Cellular processes in the developing embryo

Cellular processes characterizing each developmental stage were identified by GO terms that were overrepresented in particular coexpression modules (Figs. 3A, S5A). The early stage of Em-S1, best represented by modules DP1–DP5, was typified by overrepresentation of the GO terms Ran GTPase binding, mitotic cell cycle, nuclear division, nuclear DNA replication, cell wall organization or biogenesis, cell differentiation, mitochondrial protein complex, and tricarboxylic acid cycle. Em-S2 featured modules DP6 and DP7 that were enriched in GO terms characteristic of embryo enlargement, including cell division, cell wall organization, or biogenesis and lipid droplet. The module DP8 was characterized by up-regulation of genes involved in nutrient reservoir activity and response to external biotic stimulus, suggesting the maturation of embryo characterized by Em-S3. Stage Em-S4, represented by modules DP9–DP11, was characterized by overrepresentation of genes involved in response to biotic stimulus, structural constituent of ribosome, mitochondrial matrix, vacuole organization, and photomorphogenesis. Genes from modules DP12–DP22 were expressed broadly in the embryo across the sampled time points and were associated with protein complex, Golgi apparatus, protein kinase activity, cellular response to stimulus, RNA modification, ribosome biogenesis, and endonuclease activity.

3.3.2. Cellular processes in the developing endosperm

The functional characterization of endosperm differed from that of the embryo, as different number of modules showed a particular growth stage (Figs. 3B, S5B). Modules DP1–DP8 were characterized as the stage of En-S1, including genes involved in mitotic cell cycle, DNA replication, cell wall organization, tricarboxylic acid cycle, and starch biosynthetic process. En-S2 featured the overrepresentation of GO term nutrient reservoir activity and transporter activity in DP9. Modules DP10–DP12 showed high expression of genes involved in response to biotic stimulus and lipid storage, representing endosperm maturation at stage En-S3. Finally, module DP13 showed up-regulation of genes involved in positive regulation of autophagy, organelle disassembly, metal ion transport,

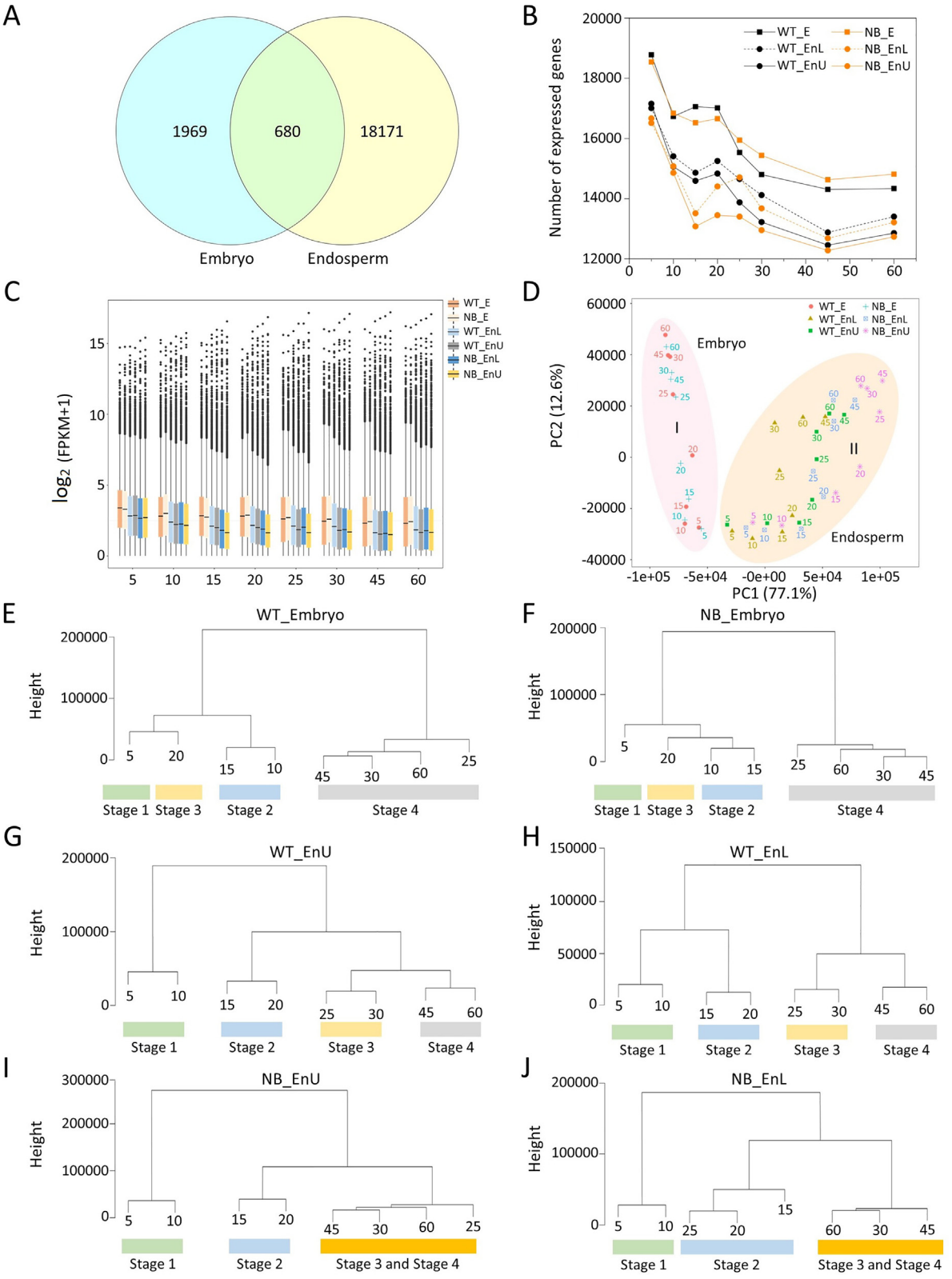

Fig. 2. Global transcriptome relationships among tissues and developmental stages. (A) Venn diagram of the 20,820 genes expressed in embryo and endosperm. (B) Number of genes detected in each tissue. (C) Comparison of gene activity between embryo and endosperm. (D) PCA of the seed tissue mRNA populations. PCA plot shows two distinct groups of embryo and endosperm mRNA populations: group I for embryo and group II for endosperm. (E) and (F) Clustered dendrogram showing global transcriptome relationships of time series samples from the embryo of WT and NB, respectively. (G) and (H) Clustered dendrogram showing global transcriptome relationships of the upper and lower endosperms of WT, respectively. (I) and (J) Clustered dendrogram showing global transcriptome relationships of the upper and lower endosperms of NB, respectively. The bottom row indicates the developmental phases according to the cluster dendrogram of the time series data. Except in (A), numbers of 5, 10, 15. . ., and 60 represent sampling timepoints (days after fertilization).

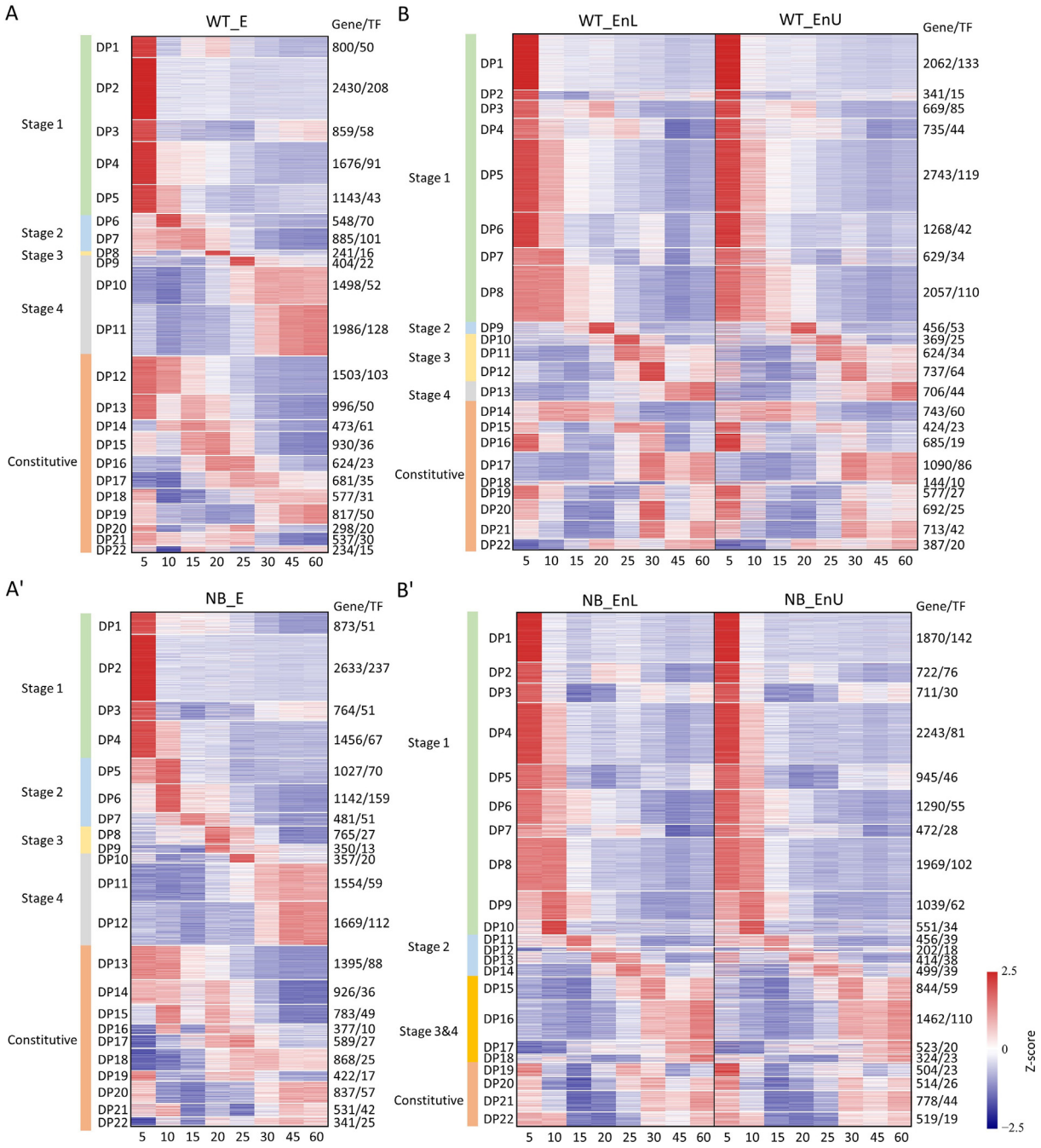

Fig. 3. Expression patterns of genes in different coexpression modules for embryo and endosperm of WT (A, B) and NB (A', B'). Coexpression modules are ordered according to the time points of their peak expression. For each gene, the FPKM value normalized by the maximum value over all time points is shown. The numbers of genes and transcription factors (TFs) in each module are shown on the right.

and cellular catabolic process, characteristic of the desiccation and dormancy stage of endosperm (En-S4). Genes responsible for metal cluster binding, macromolecular complex, RNA processing, and signal transducer activity were overrepresented in DP14–DP22 and were broadly expressed throughout development.

3.4. Metabolic dynamics of embryo and endosperm development

WT and NB shared a similar pattern of metabolic dynamics of seed development (Figs. 4 and 5). Accordingly, the normal type of WT was used for representation.

3.4.1. Sugars and starch

During embryo and endosperm development, sucrose content gradually increased, peaking at 15 DAF and decreasing thereafter (Fig. 4A, A'). Glucose and fructose levels decreased during seed development (Fig. S6A, B, A' and B'). The ratio of glucose to sucrose mediates endosperm differentiation [11]. It was higher in the embryo and endosperm at 5–10 DAF, and then decreased gradually (Fig. S6C, C'), in a manner corresponding to the transition from differentiation to storage accumulation. These sugars were unevenly distributed in rice seeds, with the embryo generally showing higher contents (Figs. 4A, A', S6A', B'). Genes participating in

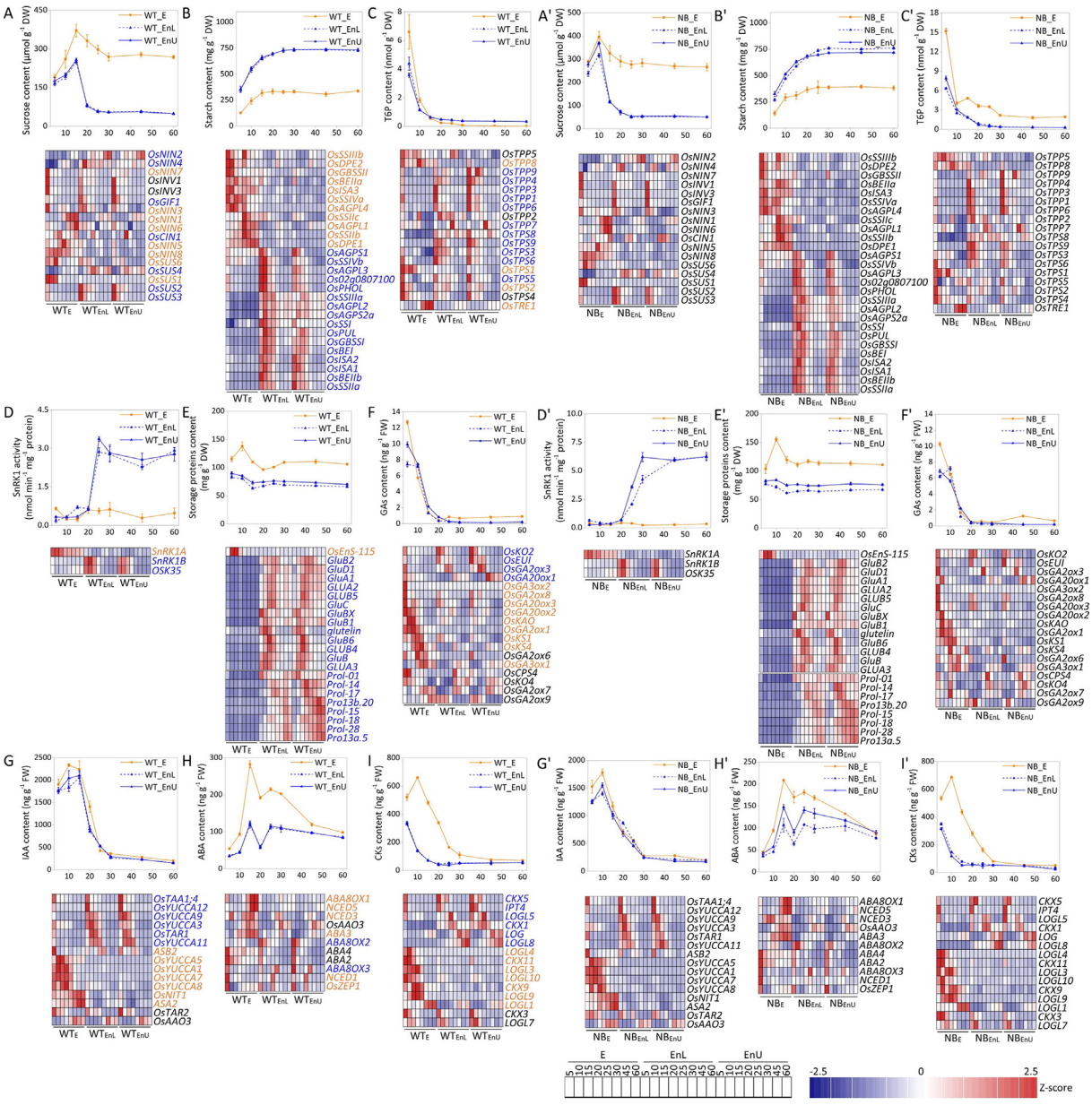

Fig. 4. Carbohydrates, proteins, SnRK1, and hormones and their regulating genes in embryo and endosperm of WT (A–I) and NB (A'–I') throughout development. Each value represents the mean ± SE of three replicates. Black, orange, and blue indicate tissue nonspecific, embryo-specific, and endosperm-specific genes, respectively.

sugar metabolism were differentially expressed between embryo and endosperm. Of the five genes encoding sucrose synthase, two (*OsSUS1* and *OsSUS6*) were expressed mainly in embryo and the other three (*OsSUS2*, *OsSUS3*, and *OsSUS4*) in endosperm (Fig. 4A, A').

During grain filling, starch content increased gradually, peaking at 20 and 30 DAF in the embryo and endosperm, respectively (Fig. 4B, B'). Compared with embryo, endosperm contained higher starch content, in agreement with a previous report [38]. Starch synthesis-associated genes were coordinately expressed in the embryo and endosperm, similarly to their expression in wheat [15]. They were expressed in endosperm primarily at 5–20 DAF. By contrast, they displayed a gradual increase in embryo at 5–20 DAF.

3.4.2. T6P and its target protein SnRK1

Trehalose-6-phospate (T6P) signals the availability of sucrose in plant cells via the feast–famine kinase, SnRK1 [39–41]. T6P levels in embryo and endosperm showed a gradual decrease in the course of development. Compared with endosperm, the embryo showed a higher content at early stage (5–10 DAF) (Fig. 4C, C'). At 5 DAF, T6P was 3.98 and 6.61 nmol g^{-1} DW in endosperm and embryo, respectively. *TPS* genes were expressed in both embryo and endosperm, predominantly at 5–20 DAF.

SnRK1 activity in endosperm maintained a low level at 5–20 DAF, and then increased rapidly at later stages (25–60 DAF). In comparison with the endosperm, SnRK1 in the embryo was at a lower level, being higher only at 5 DAF (Fig. 4D, D'). *SnRK1A* was expressed specifically in embryo, whereas two *SnRK1B* genes

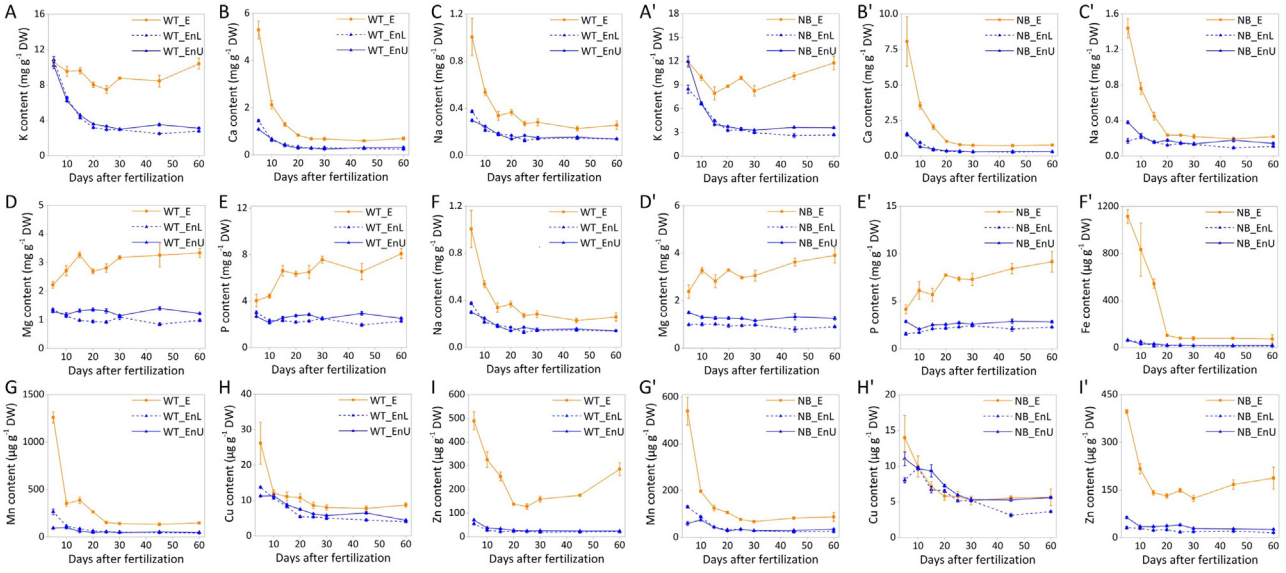

Fig. 5. Minerals in the embryo and endosperm of WT (A–I) and NB (A'–I') across developmental stages. Each value represents the mean ± SE of three replicates.

(*SnRK1B* and *OSK35*) were expressed mainly in endosperm. *SnRK1A* was broadly expressed across all time points in embryo. By contrast, *SnRK1B* and *OSK35* were more prevalent in endosperm at 5–20 DAF.

3.4.3. Amino acids and proteins

During embryo development, the level of FAAs gradually decreased at 5–25 DAF and increased thereafter (Fig. S6D, D'). In contrast, FAAs in endosperm decreased as grain filling progressed. FAAs were higher in embryo than in endosperm. Storage proteins were higher in embryo than in endosperm (Fig. 4E, E'). However, the gene expression pattern of storage protein synthesis showed a negative association with storage protein content, suggesting that their encoding genes are expressed specifically in the endosperm, as in wheat [15].

3.4.4. Phytohormones

GAs showed a gradual decrease over seed developmental course. Compared with endosperm, embryo showed higher content at 5 DAF, but showed the opposite trend at 10 DAF (Fig. 4F, F'). The GA-synthetic genes *KS* (*OsKS1* and *OsKS4*), *GA20ox* (*OsGA20ox2* and *OsGA20ox3*), and *GA3ox* (*OsGA3ox1* and *OsGA3ox2*) were expressed in embryo uniquely at 5–20 DAF, suggesting that the embryo may be the main site of GA synthesis [42,43]. Two GA-deactivating genes, *EUI* and *OsGA2ox3*, were enriched specifically in endosperm at 5 and 15–20 DAF, respectively.

Auxin gradually increased until 10–15 DAF in embryo and endosperm and decreased thereafter (Fig. 4G, G'). Compared with endosperm, embryo showed a higher content at 5–20 DAF. *OsTAA1;4* was expressed in endosperm mainly at 5 DAF.

ABA content in endosperm was half of that in embryo. It showed two peaks at 15 DAF and 25 DAF in embryo and endosperm (Fig. 4H, H'), in line with the biphasic pattern of embryonic development [44]. The activity of ABA-synthesis genes in embryo and endosperm displayed two peaks. In embryo, *NCED1*, *OsZEP1*, and *ABA2* were highly expressed at 5 DAF and *NCED3* and *NCED5* at 25 DAF. In endosperm, *NCED1*, *OsZEP1* and *ABA2* were highly expressed at 5 DAF and *NCED1* and *OsZEP1* at 20 DAF.

OsIPT4 was highly expressed at 5–10 DAF in endosperm but at 5 DAF in embryo (Fig. 4I, I'). In embryo, CKs levels gradually increased, peaked at 10 DAF, and decreased thereafter, in agreement with the expression patterns of CK-synthetic genes. The CKs in endosperm was lower than those in embryo at 5–30 DAF and peaked at 5 DAF.

3.4.5. Minerals

In embryo, contents of K, Ca, Na, Fe, Mn, Cu, and Zn decreased as development progressed, while those of Mg and P gradually increased (Fig. 5). In endosperm, contents of the nine mineral nutrients decreased as grain filling progressed, being higher at the early than at the later stage. This trend could be attributed to the dilution effect of grain dry matter, which had a higher rate of accumulation than the minerals [37]. In comparison with endosperm, the contents of all minerals were high in the embryo.

3.5. Influence of embryo on the transition of developmental stages of endosperm

3.5.1. A novel method to qualify the effect of embryo on endosperm development

As shown in Fig. 2, the duration of the middle stage in the lower part of the NB kernel (Fig. 2J) was prolonged relative to that of its upper counterpart (Fig. 2I) as well as those of the WT (Fig. 2G, H), indicating a strong influence of the embryo on the lower endosperm adjacent to it. To quantitively evaluate the embryo effect, we developed a novel comparison system by comparing the upper and lower endosperms of NB, using WT as a reference (Fig. 6).

Phenotypically, the upper and lower part of the WT endosperm look alike, whereas those of the NB endosperm are markedly different, with the upper being translucent and the lower having white belly, indicating the influence of the embryo (Fig. 1). In this study, the WT was used for estimation of the position effect (PE) between the upper and lower parts, which may be caused by factors such as the polarity development of the endosperm cells (Fig. 6A). The notched line of the NB, which is visible at 5 DAF, separates the endosperm into two mostly isolated parts. Owing to the notched line, the interface area between the upper and lower parts in NB is only 1/3 that of the WT, preventing the upper endosperm from being influenced by the endosperm. As a result, the embryo effect is trapped mainly in the lower endosperm owing to its proximity to the embryo. To compare the upper and lower endosperms, we can estimate the compound effect (CE) of the position and embryo (Fig. 6B). Finally, by elimination of the position effect, the effect

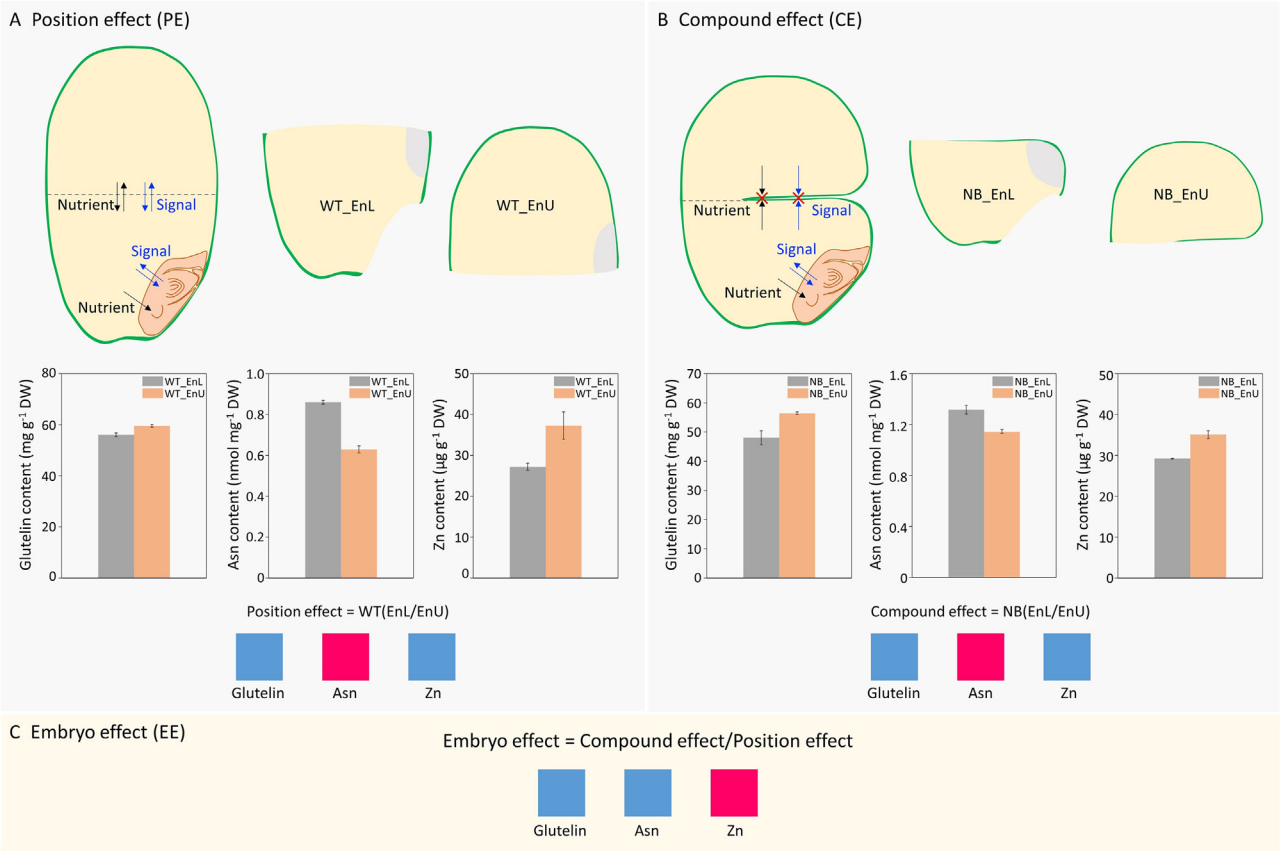

Fig. 6. Diagrammatic representation of the new comparison method for quantifying the embryo effect on endosperm development. The method has three key components: (i) Position effect (PE; A). The comparison between the upper (WT_EnU) and lower (WT_EnL) endosperms of WT reflects the difference in position between upper and lower endosperms in the WT kernel, where nutrients and signals move freely without being blocked by the notched line as in NB. (ii) Compound effect (CE; B). Owing to the notched line, movement of nutrients and signals between the two endosperms is severely restricted, trapping the influence of the embryo in the lower endosperm. Note that the 2/3 interface between the upper and lower is blocked by the notched line. Comparison between the lower part (NB_EnL) and upper part (NB_EnU) of the NB grain shows the compound effect of position and embryo. (iii) Embryo effect (EE; C). Finally, by eliminating the position effect, we can precisely calculate the influence of embryo on the endosperm via NB (EnL/EnU)/WT (EnL/EnU). Three chemical components: glutelin, Asn, and Zn, are used as examples to demonstrate the working principle of this method, as explained in detail in the main text. Red and navy blue boxes indicate up and down-regulation of glutelin, Asn, and Zn in the lower endosperm as affected by position, compound, and embryo effect, respectively.

of the embryo can be precisely estimated by further comparison of CE and PE (Fig. 6C).

To exemplify the working principle of this comparison method, we selected three metabolites including glutelin, asparagine (Asn), and Zn to show the influence of embryo (Fig. 6). First, taking into account the position and compound effects, the up-regulation of Asn and down-regulation of glutelin and Zn was observed in both genotypes. However, when the effect of position is eliminated, the embryo has a positive effect on the content of Zn and a negative effect on those of Asn and glutelin. Generally, this comparison method revealed that the position effect and the embryo effect can be either synergistic or antagonistic to the composition (Fig. 6) as well as the gene expression pattern (Fig. 7) of the endosperm.

3.5.2. T6P–SnRK1 signaling putatively mediates crosstalk between embryo and endosperm

Using the new comparison method, our results showed that the T6P–SnRK1 signaling pathway was active in the endosperm, in agreement with that of wheat [45]. As shown in Fig. 7, at the early stage of 5 to 10 DAF, the embryo showed a negative effect on sucrose, glucose, and fructose levels in endosperm during 5–10 DAF, probably owing to its nutrient consumption. The decrease of sucrose content in endosperm was accompanied by a decline in T6P levels, which abolished the inhibition of SnRK1 activity (Fig. 7A). SnRK1 promoted catabolic activity in the endosperm, as evidenced by the declining accumulation of starch and storage proteins (prolamin and glutelin), and the up-regulation of genes encoding amylase (*AMY3D*), lipase (*Os01g0651800*, *Os01g0710700*, and *Os05g0574100*), and protease (*OsSAG12* and *OsSCP28*) in endosperm. Consistently, genes participating in synthetic process of starch (*OsAGPL4*, *OsSSSIIIa*, *OsSSIVa*, *OsSSIVb*, and *Os02g0807100*) and storage protein (*OsEnS-115*, *Prol-14*, *Prol-15*, *Pro13b.20*, and *Glutelin type-B 2-like*) were all down-regulated at 5–10 DAF (Fig. 7B).

In contrast, at the middle stage between 20 and 25 DAF, T6P–SnRK1 signaling showed a trend opposite to that at 5–10 DAF. Gene activities of sucrose metabolism (*OsINV1* and *OsNIN6*) and T6P synthesis (*OsTPS9* and *Os08g0414700*) were up-regulated (Fig. 7). SnRK1 activity was inhibited synchronously in endosperm (Fig. 7A). Starch synthetic process was promoted and catabolic processes were inhibited by SnRK1, as reflected by the overrepresented starch-synthetic genes (*OsAGPL3* and *ISA1*) and underrepresented catabolic genes encoding amylase (*AMY3A* and *AMY3E*), and protease (*OsAP1*, *Os04g0535200*, *Os08g0267300*, *Os05g0403000*, *Os04g0330900*, and *OsSAG12-1*) in endosperm (Fig. 7B).

This comparison method revealed that the influence of embryo on IAA was similar to that of T6P but contrary to SnRK1 activity across the developmental stages, decreasing at 10 DAF while

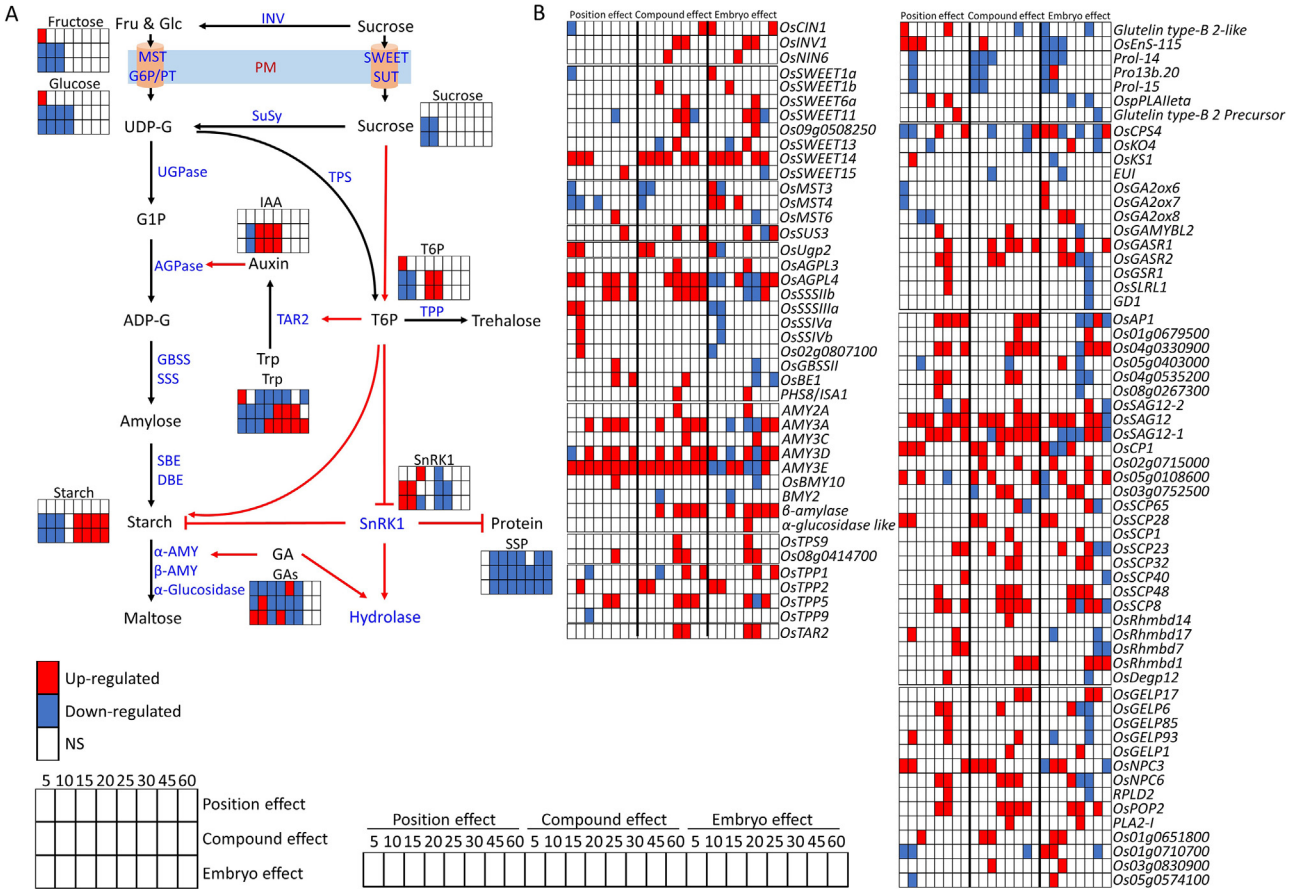

Fig. 7. Putative role of T6P–SnRK1 signaling in developmental transition of the endosperm as revealed by the proposed new comparison method. Effects of position, compound, and embryo are all shown. (A) Schematic diagram showing the putative T6P–SnRK1 signaling pathway. (B) Heat map of differentially expressed genes associated with position, compound, and embryo effects. ADP-G, ADP-glucose; AGPase, ADP-glucose pyrophosphorylase; DBE, debranching enzyme; Fru, fructose; G6P/PT, glucose-6-phosphate/phosphate translocator; G1P, glucose 1-phosphate; GA, gibberellin; GBSS, granule-bound starch synthase; Glc, glucose; IAA, indoleacetic acid; INV, invertase; ISA, isoamylase; MST, monosaccharide transporter; PM, plasm membrane; SBE, starch branching enzyme; SnRK1, sucrose non-fermenting-1 related protein kinase 1; SSP, seed storage protein; SSS, soluble starch synthase; SuSy, sucrose synthase; SUT, sucrose transporter; T6P, trehalose 6-phosphate; TAR2, tryptophan aminotransferase 2; TPP, trehalose 6-phosphate phosphatase; TPS, trehalose 6-phosphate synthase; Trp, tryptophan; UDP-G, UDP-glucose; UGPase, UDP-glucose pyrophosphorylase; α-AMY, α-amylase; β-AMY, β-Amylase. Red and navy rectangles indicate up- and down-regulation, respectively.

increasing at 15–25 DAF (Fig. 7A). Recently, by modulating T6P content in growing embryos of garden pea (*Pisum sativum*), Meitzel et al. [46] found that auxin acts downstream of T6P to facilitate seed filling. Our finding of the synchronously dynamic pattern of IAA and T6P indicates a similar role of auxin–T6P pathway in the grain-filling process of rice.

4. Discussion

This study took advantage of the NB mutant to evolve a novel comparison method for quantifying the influence of embryo on endosperm development, revealing that the embryo has a dragging effect on the developmental transition of the endosperm. To our knowledge, this is the first attempt to characterize the evidence of embryo–endosperm interaction during rice seed development. The findings reveal new aspects of the role of embryo in the formation process of rice quality, and help to draw an integrative picture of seed development from the perspective of agronomy and crop physiology.

4.1. The dragging effect of embryo on endosperm development

Seed development is an orchestrated progression through a series of stages, which can be described by two types of time: chronological time and developmental time defined by the sequence of stages [47]. There is evidence of bidirectional interaction between embryo and endosperm throughout development [1]. Two recent studies in *Arabidopsis* suggest an independent relationship between the two tissues. By analyzing mutants with defective endosperm cellularization, O'Neill et al. [48] found that this endosperm process is not required for the onset of embryo maturation. Using single-fertilization mutants, Xiong et al. [49] demonstrated that in the absence of embryo, endosperm develops in the same manner as in the wild type, suggesting that endosperm development is an autonomously programmed process independent of embryogenesis. These two studies in combination indicate that in terms of developmental time, the mechanisms controlling endosperm and embryo development act independently of each other [48]. In contrast, in terms of chronological time, the present study showed that duration of endosperm filling in the lower part of NB kernels was prolonged by the embryo (Fig. 2J), suggesting a substantial interaction between embryo and endosperm. Similarly, Xiong et al. [49] showed that rapid embryo expansion accelerated endosperm breakdown, shortening the lifespan of the transient endosperm. Cereal seeds like rice have a persistent endosperm, whereas dicots like *Arabidopsis* have an ephemeral endosperm that degrades as the embryo grows. Whether the independence of endosperm development from embryo in *Arabidopsis* is applicable to rice awaits further investigation.

Plants have evolved a variety of timing mechanisms that integrate chronological time with developmental time to ensure proper development [48]. For the endosperm, these include internal timers of molecular oscillators based on hormones or metabolites, and external timers dependent on environmental signals or emanating from a different tissue like the embryo. This study reveals a dragging effect of embryo on endosperm development in chronological time, extending the storage accumulating stage but delaying the maturation stage. This finding provides direct evidence for the role of the embryo as an external timer controlling endosperm development. The hormones GA, auxins, and ABA were unevenly distributed in rice seed, with the embryo generally showing higher contents at the early and middle stages, as also reported by Zhang et al. [43]. *GA20ox* (*GA20ox2* and *GA20ox3*), *GA3ox* (*OsGA3ox1* and *OsGA3ox2*), *KS* (*OsKS1* and *OsKS4*) were expressed in embryo predominantly at 5–20 DAF, suggesting that the embryo may be the GA-synthetic site and the endosperm the GA-acting site (Fig. 4F). It is well established that embryo-derived GA modulates the secretion of starch-degrading enzymes such as α-amylase from the aleurone and scutellum upon germination. But it is still uncertain whether the degradation of starch during seed development is analogous to the germination process [3]. Our results suggest that one of the external timers coordinating rice grain development is the hormone GA released from endosperm.

For internal timers modifying endosperm development, the T6P–SnRK1 signaling pathway may be the key component. At the early stage of 5–10 DAF, sucrose in endosperm was lower, probably owing to deprivation by the growing embryo. In response to the reduced sucrose content, T6P decreased simultaneously in endosperm, relieving the inhibition of SnRK1 activity. The increased SnRK1 activities promoted the catabolism or suppressed the anabolism of starch and proteins, as reflected by the lower content of starch and prolamins as well as the increased gene activity of amylase, lipase, and protease in endosperm (Fig. 7). In contrast, at the middle stage between 20 and 25 DAF, T6P–SnRK1 signaling showed a trend opposite to that between 5 and 10 DAF, suggesting that it may be involved in transition between developmental stages in endosperm (Fig. 7). The anticorrelation between T6P and SnRK1 activity opens the possibility that the T6P–SnRK1 pathway is a master regulator coordinating the communication between embryo and endosperm during rice grain formation.

4.2. The integrative landscape of rice seed development

One of the major goals of crop production is to produce more grain with less time, thus increasing resource-use efficiency. The duration of each stage of seed development and the timing of transition between them is of agronomical significance. As reviewed by Olsen [11], the mechanism regulating the timing of endosperm cellularization has attracted attention owing to its positive association with endosperm and seed size. Consequently, a precise and integrative landscape of seed development is necessary and will be useful for both fundamental and applied studies on the mechanisms underpinning crop yield and quality. Previously, from the viewpoint of crop physiology, we proposed a practical staging system with three phases: embryo morphogenesis, endosperm filling, and seed maturation [1]. Here, we update this staging system by integrating molecular, physiological, and anatomical evidence from the present study as well as from the literature. In particular, considering the dragging effect of embryo on endosperm development at the former second stage (endosperm filling), we highlight the importance of this stage as critical for grain filling and quality formation, and thus subdivide it into two stages: embryo enlargement and endosperm filling. We paint a holistic and dynamic picture of rice seed development (Fig. 8), and provide a brief description of each stage and its agronomical relevance as follows.

Stage I, morphogenesis (0–10 DAF). After double fertilization, patterning and differentiation occur simultaneously in the embryo and endosperm. At the end of this stage, most of the morphogenetic events in embryo have occurred. The endosperm has finished differentiation, forming two subregions, the aleurone and starchy endosperm, and begins to store starch and proteins. This stage is crucial for embryo morphogenesis and is also critical for endosperm development, as evidenced by the highly expressed *Chalk5* gene, which is responsible for the formation of chalkiness [50].

Stage II, embryo enlargement (10–20 DAF). The embryo grows to its maximum volume at 20 DAF [51]. Starchy endosperm attains its highest rate of storage accumulation [52,53], while aleurone cells are filled with aleurone particles and spherosomes at the end of this stage [54]. This stage witnesses strong interactions between embryo and endosperm and is thus critical for rice grain filling and quality. As reported by Morita et al. [55] and Shi et al. [56], heat stress caused rapid proliferation and expansion of endosperm cells. The resulting high incidence of chalky tissue was considered to be associated with the incomplete accumulation of starch that cannot completely fill the increased endosperm cells. In contrast, our present findings indicate that the slowdown of endosperm development is another cause of chalkiness formation. It may thus be inferred that a perfect rice kernel without chalky tissue demands a delicate balance between the enlargement of endosperm size and the accumulation of storage products. For this reason, the timing of the transition from cell differentiation to storage accumulation is critical for the formation of grain chalkiness. The role of the embryo in this transitional process requires further investigation.

Stage III, endosperm filling (20–30 DAF). The embryo becomes dormant and the endosperm continues to accumulate starch and proteins, reaching its maximum weight at 30 DAF. By the end of this stage, most of the starchy endosperm and maternal tissues have undergone programmed cell death, losing their biological activity, while the aleurone and embryo are still alive [57,58]. This is another important stage for the formation of grain yield (weight). However, little information concerning the cellular events at this stage is available, especially for the role of the mature embryo in regulating endosperm filling.

Stage IV, maturation (30 DAF-maturity). After completion of reserve accumulation, the embryo becomes tolerant of desiccation, and undergoes a developmentally programmed dehydration event leading to dormancy and a quiescent state [59,60]. The starchy endosperm cells die completely upon seed maturation and desiccation. This stage lasts for 20 to 40 days with no marked increase in grain weight. Seeds are susceptible to germination under hot and humid conditions, thus being vulnerable to preharvest sprouting [61]. It is still unknown whether there is an embryo–endosperm interaction at the late stage of grain filling.

Fig. 8 draws distinctive patterns of embryo and endosperm development, with the endosperm ceasing storage accumulation at 30 DAF, ten days after the corresponding timepoint of the embryo (20 DAF). Fig. S7 shows that the capacity of the embryo to germinate starts at 15 DAF and peaks at 20 DAF for both genotypes, WT and NB. It may thus be inferred that the embryo has the priority of nutrient allocation over endosperm during seed development. Moreover, it appears that this asynchrony of embryo and endosperm development is conserved across modern cultivars. They share a common chronological time, with embryo developmentally maturing at 20 DAF [62,63], while endosperm matures at 30 DAF [55,58,64–68]. Thus, the essential period of rice yield and quality formation is in stages I–III (Fig. 8), from anthesis to 30 DAF. After that, rice seed enters the stage of desiccation and

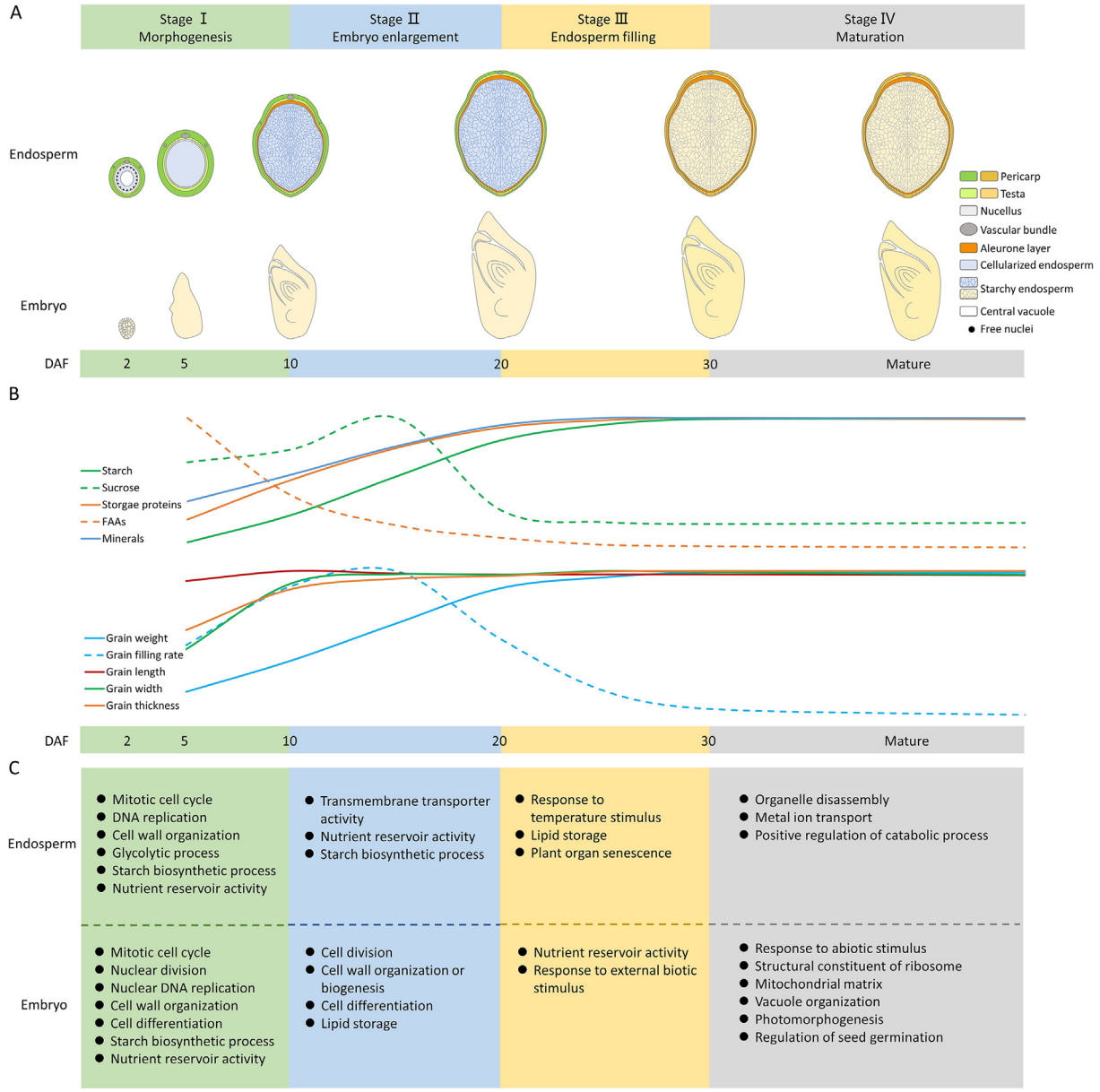

Fig. 8. Holistic and dynamic picture of seed development. (A) Schematic illustration of the morphological changes in embryo (longitudinal section) and endosperm (transverse). Varying colors of the pericarp and testa show the progression of degradation in maternal tissues, while those of the starch endosperm show the grain-filling process. (B) Dynamic accumulation of storage materials (sucrose, starch, FAAs, storage proteins, and minerals) and increases in grain weight, length, width, and thickness. (C) Molecular signatures of the embryo and endosperm at different developmental stages.

maturation, which lasts 20–40 days with no marked increase in grain weight. By dividing the 60-day period of grain filling into two separate months, our previous report showed that only 10% of the grain yield was formed after 30 DAF [68]. Under the intensive rice–wheat and rice–oilseed rape cropping systems in the lower Yangtze River, China, late maturity of the rice crop results in late sowing of wheat and oilseed rape, impairing seedling growth and consequently grain or seed yield [69,70]. We suggest genetic intervention to shorten the duration of the late maturation stage of rice for adaptation to the double cropping systems. Future work should exploit more genotypes to verify that this asynchrony of embryo and endosperm development in chronological time is conserved in rice as well as in other cereal crops such as maize and wheat.

5. Conclusions

We applied a novel comparison method based on the NB mutant, demonstrating a direct effect of the embryo on the developmental processes of the endosperm. Integrated analysis of transcriptome and metabolites identified putative regulatory timers that coordinate the developmental process between embryo and endosperm. The external timers for endosperm may be hormones such as GA secreted from the embryo, while the internal timer may be the T6P–SnRK1 signaling pathway that mediates carbon allocation in endosperm. In combination with results from molecular, physiological, and anatomical investigations, we proposed a holistic and dynamic landscape of rice seed development, and explained its agronomical significance, in particular for the

intensive systems of rice–wheat or rice–oilseed rape double cropping. The integrative picture of rice grain formation proposed here seeks to bridge the knowledge gap between the fundamental science of genetic control of seed development and the applied sciences such as the physiology of grain filling and quality, and will facilitate the design of strategies to enhance rice yield and quality.

CRediT authorship contribution statement

Yang Tao: Investigation, Data curation, Formal analysis, Validation, Visualization, Writing – original draft, Writing – review & editing. **Lu An:** Formal analysis, Visualization, Writing – original draft. **Feng Xiao:** Investigation. **Ganghua Li:** Writing – review & editing, Funding acquisition. **Yanfeng Ding:** Writing – review & editing, Funding acquisition. **Matthew J. Paul:** Writing – review & editing, Funding acquisition. **Zhenghui Liu:** Conceptualization, Supervision, Project administration, Methodology, Writing – original draft, Writing – review & editing, Funding acquisition.

Declaration of competing interest

The authors declare that they have no known competing financial interests or personal relationships that could have appeared to influence the work reported in this paper.

Acknowledgments

The research was supported by the National Key Research and Development Program of China (2017YFD0300103), the National Natural Science Foundation of China (31771719), and the National High Technology Research and Development Program of China (2014AA10A605). Rothamsted Research receives strategic funding from the Biotechnological and Biological Sciences Research Council of the UK. Matthew J. Paul acknowledges funding from the Designing Future Wheat Strategic Program (BB/P016855/1).

Data availability statement

All the analyzed data relevant to this manuscript are present in this paper and its supplementary data. All the raw data associated with this study have been submitted to NCBI and are available under accession number PRJNA722833.

Appendix A. Supplementary data

Supplementary data for this article can be found online at https://doi.org/10.1016/j.cj.2021.10.007.

References

[1] L. An, Y. Tao, H. Chen, M.J. He, F. Xiao, G.H. Li, Y.F. Ding, Z.H. Liu, Embryo-endosperm interaction and its agronomic relevance to rice quality, Front. Plant Sci. 11 (2020) 587641.
[2] T.Y. Wu, M. Müller, W. Gruissem, N.K. Bhullar, Genome wide analysis of the transcriptional profiles in different regions of the developing rice grains, Rice 13 (2020) 62.
[3] N. Sreenivasulu, V.M. Butardo, G. Misra, R.P. Cuevas, R. Anacleto, P.B.K. Kishor, Designing climate-resilient rice with ideal grain quality suited for high-temperature stress, J. Exp. Bot. 66 (2015) 1737–1748.
[4] M. Xi, Z. Lin, X. Zhang, Z. Liu, G. Li, Q. Wang, S. Wang, Y. Ding, Endosperm structure of white-belly and white-core rice grains shown by scanning electron microscopy, Plant Prod. Sci. 17 (2014) 285–290.
[5] M.A. Fitzgerald, S.R. McCouch, R.D. Hall, Not just a grain of rice: the quest for quality, Trends Plant Sci. 14 (2009) 133–139.
[6] Z.M. Lin, Z.X. Wang, X.C. Zhang, Z.H. Liu, G.H. Li, S.H. Wang, Y.F. Ding, Complementary proteome and transcriptome profiling in developing grains of a notched-belly rice mutant reveals key pathways involved in chalkiness formation, Plant Cell Physiol. 58 (2017) 560–573.
[7] T. Ishimaru, S. Parween, Y. Saito, T. Shigemitsu, H. Yamakawa, M. Nakazono, T. Masumura, N.K. Nishizawa, M. Kondo, N. Sreenivasulu, Laser microdissection-based tissue-specific transcriptome analysis reveals a novel regulatory network of genes involved in heat-induced grain chalk in rice endosperm, Plant Cell Physiol. 60 (2019) 626–642.
[8] C. Lafon-Placette, C. Köhler, Embryo and endosperm, partners in seed development, Curr. Opin. Plant Biol. 17 (2014) 64–69.
[9] N.M. Doll, J. Just, V. Brunaud, J. Caïus, A. Grimault, N. Depège-Fargeix, E. Esteban, A. Pasha, N.J. Provart, G.C. Ingram, P.M. Rogowsky, T. Widiez, Transcriptomics at maize embryo/endosperm interfaces identifies a transcriptionally distinct endosperm subdomain adjacent to the embryo scutellum, Plant Cell 32 (2020) 833–852.
[10] G.C. Ingram, Family plot: The impact of the endosperm and other extra-embryonic seed tissues on angiosperm zygotic embryogenesis, F1000Research 9 (2020) 18.
[11] O.A. Olsen, The modular control of cereal endosperm development, Trends Plant Sci. 25 (2020) 279–290.
[12] M.F. Belmonte, R.C. Kirkbride, S.L. Stone, J.M. Pelletier, A.Q. Bui, E.C. Yeung, M. Hashimoto, J. Fei, C.M. Harada, M.D. Munoz, B.H. Le, G.N. Drews, S.M. Brady, R. B. Goldberg, J.J. Harada, Comprehensive developmental profiles of gene activity in regions and subregions of the *Arabidopsis* seed, Proc. Natl. Acad. Sci. U. S. A. 110 (2013) E435–E444.
[13] J. Chen, B. Zeng, M. Zhang, S.J. Xie, G.K. Wang, A. Hauck, J.S. Lai, Dynamic transcriptome landscape of maize embryo and endosperm development, Plant Physiol. 166 (2014) 252–264.
[14] F. Yi, W. Gu, J. Chen, N. Song, X. Gao, X. Zhang, Y. Zhou, X. Ma, W. Song, H. Zhao, E. Esteban, A. Pasha, N.J. Provart, J. Lai, High temporal-resolution transcriptome landscape of early maize seed development, Plant Cell 31 (2019) 974–992.
[15] D. Xiang, T.D. Quilichini, Z. Liu, P. Gao, Y. Pan, Q. Li, K.T. Nilsen, P. Venglat, E. Esteban, A. Pasha, Y. Wang, R. Wen, Z. Zhang, Z. Hao, E. Wang, Y. Wei, R. Cuthbert, L.V. Kochian, A. Sharpe, N. Provart, D. Weijers, C.S. Gillmor, C. Pozniak, R. Datla, The transcriptional landscape of polyploid wheats and their diploid ancestors during embryogenesis and grain development, Plant Cell 31 (2019) 2888–2911.
[16] J.X. Bian, P.C. Deng, H.S. Zhan, X.T. Wu, M.D.L.C. Nishantha, Z.G. Yan, X.H. Du, X. J. Nie, W.N. Song, Transcriptional dynamics of grain development in barley (*Hordeum vulgare* L.), Int. J. Mol. Sci. 20 (2019) 1–16.
[17] H. Ram, A. Singh, M. Katoch, R. Kaur, S. Sardar, S. Palia, R. Satyam, H. Sonah, R. Deshmukh, A.K. Pandey, I. Gupta, T.R. Sharma, Dissecting the nutrient partitioning mechanism in rice grain using spatially resolved gene expression profiling, J. Exp. Bot. 72 (2021) 2212–2230.
[18] X.H. Tong, Y.F. Wang, A.Q. Sun, B.K. Bello, S. Ni, J. Zhang, *Notched belly grain 4*, a novel allele of *dwarf 11*, regulates grain shape and seed germination in rice (*Oryza sativa* L.), Int. J. Mol. Sci. 19 (2018) 4069.
[19] Z.M. Lin, X.C. Zhang, X.Y. Yang, G.H. Li, S. Tang, S.H. Wang, Y.F. Ding, Z.H. Liu, Proteomic analysis of proteins related to rice grain chalkiness using iTRAQ and a novel comparison system based on a notched-belly mutant with white-belly, BMC Plant Biol. 14 (2014) 163.
[20] Z. Lin, D. Zheng, X. Zhang, Z. Wang, J. Lei, Z. Liu, G. Li, S. Wang, Y. Ding, Chalky part differs in chemical composition from translucent part of *japonica* rice grains as revealed by a notched-belly mutant with white-belly, J. Sci. Food Agric. 96 (2016) 3937–3943.
[21] Y.X. Chen, Y.S. Chen, C.M. Shi, Z.B. Huang, Y. Zhang, S.K. Li, Y. Li, J. Ye, C. Yu, Z. Li, X.Q. Zhang, J. Wang, H.M. Yang, L. Fang, Q. Chen, SOAPnuke: a MapReduce acceleration-supported software for integrated quality control and preprocessing of high-throughput sequencing data, GigaScience 7 (2018) 1–6.
[22] A.M. Bolger, M. Lohse, B. Usadel, Trimmomatic: a flexible trimmer for Illumina sequence data, Bioinformatics 30 (2014) 2114–2120.
[23] D. Kim, B. Langmead, S.L. Salzberg, HISAT: A fast spliced aligner with low memory requirements, Nat. Methods 12 (2015) 357–360.
[24] B. Li, C.N. Dewey, RSEM: accurate transcript quantification from RNA-Seq data with or without a reference genome, BMC Bioinformatics 12 (2011) 323.
[25] L.K. Wang, Z.X. Feng, X. Wang, X.W. Wang, X.G. Zhang, DEGseq: an R package for identifying differentially expressed genes from RNA-seq data, Bioinformatics 26 (2009) 136–138.
[26] Z.W. An, Y.H. Zhao, H. Cheng, W.G. Li, H.S. Huang, Development and application of EST-SSR markers in *Hevea brasiliensis* Muell, Hereditas 31 (2009) 311–319 (in Chinese with English abstract).
[27] E. Howe, K. Holton, S. Nair, D. Schlauch, R. Sinha, J. Quackenbush, MeV: multi experiment viewer, in: M.F. Ochs, J.T. Casagrande, R.V. Davuluri (Eds.), Biomedical Informatics for Cancer Research, Springer, Boston, USA, 2010, pp. 267–277.
[28] M. Ashburner, C.A. Ball, J.A. Blake, D. Botstein, H. Butler, J.M. Cherry, A.P. Davis, K. Dolinski, S.S. Dwight, J.T. Eppig, M.A. Harris, D.P. Hill, L. Issel-Tarver, A. Kasarskis, S. Lewis, J.C. Matese, J.E. Richardson, M. Ringwald, G.M. Rubin, G. Sherlock, The Gene Ontology Consortium, Gene ontology: tool for the unification of biology, Nat. Genet. 25 (2000) 25–29.
[29] R.C. Team, R: A Language and Environment for Statistical Computing, R Foundation for Statistical Computing, Vienna, Austria, 2013.
[30] P.F. Chen, L. Chen, Z.R. Jiang, G.P. Wang, S.H. Wang, Y.F. Ding, Sucrose is involved in the regulation of iron deficiency responses in rice (*Oryza sativa* L.), Plant Cell Rep. 37 (2018) 789–798.
[31] T.L. Delatte, M.H.J. Selman, H. Schluepmann, G.W. Somsen, S.C.M. Smeekens, G. J. de Jong, Determination of trehalose-6-phosphate in *Arabidopsis* seedlings by successive extractions followed by anion exchange chromatography-mass spectrometry, Anal. Biochem. 389 (2009) 12–17.
[32] J. Sastre Toraño, T.L. Delatte, H. Schluepmann, S.C.M. Smeekens, G.J. de Jong, G. W. Somsen, Determination of trehalose-6-phosphate in *Arabidopsis thaliana*

seedlings by hydrophilic-interaction liquid chromatography-mass spectrometry, Anal. Bioanal. Chem. 403 (2012) 1353–1360.
[33] Y.H. Zhang, L.F. Primavesi, D. Jhurreea, P.J. Andralojc, R.A.C. Mitchell, S.J. Powers, H. Schluepmann, T. Delatte, A. Wingler, M.J. Paul, Inhibition of SNF1-related protein kinase1 activity and regulation of metabolic pathways by trehalose-6-phosphate, Plant Physiol. 149 (2009) 1860–1871.
[34] H. Ning, J. Qiao, Z. Liu, Z. Lin, G. Li, Q. Wang, S. Wang, Y. Ding, Distribution of proteins and amino acids in milled and brown rice as affected by nitrogen fertilization and genotype, J. Cereal Sci. 52 (2010) 90–95.
[35] C. Wu, K.H. Cui, W.C. Wang, Q. Li, S. Fahad, Q.Q. Hu, J.L. Huang, L.X. Nie, S.B. Peng, Heat-induced phytohormone changes are associated with disrupted early reproductive development and reduced yield in rice, Sci. Rep. 6 (2016) 34978.
[36] C.C. Chou, W.S. Chen, K.L. Huang, H.C. Yu, L.J. Liao, Changes in cytokinin levels of *Phalaenopsis* leaves at high temperature, Plant Physiol. Biochem. 38 (2000) 309–314.
[37] Z. Wang, F. Zhang, F. Xiao, Y. Tao, Z. Liu, G. Li, S. Wang, Y. Ding, Contribution of mineral nutrients from source to sink organs in rice under different nitrogen fertilization, Plant Growth Regul. 86 (2018) 159–167.
[38] B.O. Juliano, D.B. Bechtel, The rice grain and its gross composition, in: B.O. Juliano (Ed.), Rice: Chemistry and Technology, American Association of Cereal Chemistry, St. Paul, MN, USA, 1985, pp. 17–57.
[39] M. Dingkuhn, D. Luquet, D. Fabre, B. Muller, X. Yin, M.J. Paul, The case for improving crop carbon sink strength or plasticity for a CO_2-rich future, Curr. Opin. Plant Biol. 56 (2020) 259–272.
[40] L.E. O'Hara, M.J. Paul, A. Wingler, How do sugars regulate plant growth and development? New insight into the role of trehalose-6-phosphate, Mol. Plant 6 (2013) 261–274.
[41] M.J. Paul, M. Oszvald, C. Jesus, C. Rajulu, C.A. Griffiths, Increasing crop yield and resilience with trehalose 6-phosphate: targeting a feast-famine mechanism in cereals for better source-sink optimization, J. Exp. Bot. 68 (2017) 4455–4462.
[42] L.J. Xue, J.J. Zhang, H.W. Xue, Genome-wide analysis of the complex transcriptional networks of rice developing seeds, PLoS ONE 7 (2012) e31081.
[43] X.F. Zhang, J.H. Tong, A.N. Bai, C.M. Liu, L.T. Xiao, H.W. Xue, Phytohormone dynamics in developing endosperm influence rice grain shape and quality, J. Integr. Plant Biol. 62 (2020) 1625–1637.
[44] Z.Z. Qin, X.H. Tang, G.Z. Pan, M.Y. He, Changes of endogenous ABA levels in rice embryo and endosperm and association with development and germination, J. Integr. Plant Biol. 32 (1990) 448–455 (in Chinese with English abstract).
[45] E. Martínez-Barajas, T. Delatte, H. Schluepmann, G.J. de Jong, G.W. Somsen, C. Nunes, L.F. Primavesi, P. Coello, R.A.C. Mitchell, M.J. Paul, Wheat grain development is characterized by remarkable trehalose 6-phosphate accumulation pregrain filling: tissue distribution and relationship to SNF1-related protein kinase1 activity, Plant Physiol. 156 (2011) 373–381.
[46] T. Meitzel, R. Radchuk, E.L. McAdam, I. Thormählen, R. Feil, E. Munz, A. Hilo, P. Geigenberger, J.J. Ross, J.E. Lunn, L. Borisjuk, Trehalose 6-phosphate promotes seed filling by activating auxin biosynthesis, New Phytol. 229 (2021) 1553–1565.
[47] M. Ebisuya, J. Briscoe, What does time mean in development? Development 145 (2018) dev164368.
[48] J.P. O'Neill, K.T. Colon, P.D. Jenik, The onset of embryo maturation in *Arabidopsis* is determined by its developmental stage and does not depend on endosperm cellularization, Plant J. 99 (2019) 286–301.
[49] H.X. Xiong, W. Wang, M.X. Sun, Endosperm development is an autonomously programmed process independent of embryogenesis, Plant Cell 33 (2021) 1151–1160.
[50] Y. Li, C. Fan, Y. Xing, P. Yun, L. Luo, B. Yan, B.O. Peng, W. Xie, G. Wang, X. Li, J. Xiao, C. Xu, Y. He, *Chalk5* encodes a vacuolar H^+-translocating pyrophosphatase influencing grain chalkiness in rice, Nat. Genet. 46 (2014) 398–404.
[51] J.I. Itoh, K.I. Nonomura, K. Ikeda, S. Yamaki, Y. Inukai, H. Yamagishi, H. Kitano, Y. Nagato, Rice plant development: from zygote to spikelet, Plant Cell Physiol. 46 (2005) 23–47.
[52] G.H. Zhu, N.H. Ye, J.C. Yang, X.X. Peng, J.H. Zhang, Regulation of expression of starch synthesis genes by ethylene and ABA in relation to the development of rice inferior and superior spikelets, J. Exp. Bot. 62 (2011) 3907–3916.
[53] J. Fu, Y.J. Xu, L.U. Chen, L.M. Yuan, Z.Q. Wang, J.C. Yang, Changes in enzyme activities involved in starch synthesis and hormone concentrations in superior and inferior spikelets and their association with grain filling of super rice, Rice Sci. 20 (2013) 120–128.
[54] X.R. Yu, L. Zhou, F. Xiong, Z. Wang, Structural and histochemical characterization of developing rice caryopsis, Rice Sci. 21 (2014) 142–149.
[55] S. Morita, J.I. Yonemaru, J.I. Takanashi, Grain growth and endosperm cell size under high night temperatures in rice (*Oryza sativa* L.), Ann. Bot. 95 (2005) 695–701.
[56] W.J. Shi, X.Y. Yin, P.C. Struik, C. Solis, F.M. Xie, R.C. Schmidt, M. Huang, Y.B. Zou, C. R. Ye, S.V.K. Jagadish, High day- and night-time temperatures affect grain growth dynamics in contrasting rice genotypes, J. Exp. Bot. 68 (2017) 5233–5245.
[57] X. Wu, J. Liu, D. Li, C.M. Liu, Rice caryopsis development I: dynamic changes in different cell layers, J. Integr. Plant Biol. 58 (2016) 772–785.
[58] X. Wu, J. Liu, D. Li, C.M. Liu, Rice caryopsis development II: dynamic changes in the endosperm, J. Integr. Plant Biol. 58 (2016) 786–798.
[59] R. Angelovici, G. Galili, A.R. Fernie, A. Fait, Seed desiccation: a bridge between maturation and germination, Trends Plant Sci. 15 (2010) 211–218.
[60] A.J. Manfre, G.A. LaHatte, C.R. Climer, W.R. Marcotte, Seed dehydration and the establishment of desiccation tolerance during seed maturation is altered in the *Arabidopsis thaliana* mutant *atem6-1*, Plant Cell Physiol. 50 (2009) 243–253.
[61] L. Du, F. Xu, J. Fang, S. Gao, J. Tang, S. Fang, H. Wang, H. Tong, F. Zhang, J. Chu, G. Wang, C. Chu, Endosperm sugar accumulation caused by mutation of *PHS8*/*ISA1* leads to pre-harvest sprouting in rice, Plant J. 95 (2018) 545–556.
[62] A. Armenta-Medina, C.S. Gillmor, P. Gao, J. Mora-Macias, L.V. Kochian, D. Xiang, R. Datla, Developmental and genomic architecture of plant embryogenesis: from model plant to crops, Plant Commun. 2 (2021) 100136.
[63] J.I. Itoh, Y. Sato, Y. Sato, K.I. Hibara, S. Shimizu-Sato, H. Kobayashi, H. Takehisa, K.A. Sanguinet, N. Namiki, Y. Nagamura, Genome-wide analysis of spatiotemporal gene expression patterns during early embryogenesis in rice, Development 143 (2016) 1217–1227.
[64] J.C. Yang, J.H. Zhang, Z.Q. Wang, K. Liu, P. Wang, Post-anthesis development of inferior and superior spikelets in rice in relation to abscisic acid and ethylene, J. Exp. Bot. 57 (2006) 149–160.
[65] E. Wang, J. Wang, X. Zhu, W. Hao, L. Wang, Q. Li, L. Zhang, W. He, B. Lu, H. Lin, H. Ma, G. Zhang, Z. He, Control of rice grain-filling and yield by a gene with a potential signature of domestication, Nat. Genet. 40 (2008) 1370–1374.
[66] T.T. Chen, Y.J. Xu, J.C. Wang, Z.Q. Wang, J.C. Yang, J.H. Zhang, Polyamines and ethylene interact in rice grains in response to soil drying during grain filling, J. Exp. Bot. 64 (2013) 2523–2538.
[67] X. Wei, G. Jiao, H. Lin, Z. Sheng, G. Shao, L. Xie, S. Tang, Q. Xu, P. Hu, *GRAIN INCOMPLETE FILLING 2* regulates grain filling and starch synthesis during rice caryopsis development, J. Integr. Plant Biol. 59 (2017) 134–153.
[68] H.F. Xu, Z.X. Wang, F. Xiao, L. Yang, G.H. Li, Y.F. Ding, M.J. Paul, W.W. Li, Z.H. Liu, Dynamics of dry matter accumulation in internodes indicates source and sink relations during grain-filling stage of *japonica* rice, Field Crops Res. 263 (2021) 108009.
[69] H. Bai, F. Tao, Sustainable intensification options to improve yield potential and eco-efficiency for rice-wheat rotation system in China, Field Crops Res. 211 (2017) 89–105.
[70] Z. Zhang, R.H. Cong, T. Ren, H. Li, Y. Zhu, J.W. Lu, Optimizing agronomic practices for closing rapeseed yield gaps under intensive cropping systems in China, J. Integr. Agric. 19 (2020) 1241–1249.